



DIRECT TORQUE CONTROL BASED ON SPACE VECTOR MODULATION WITH BALANCING STRATEGY OF DUAL STAR INDUCTION MOTOR

ELAKHDAR BENYOUSSEF¹, SAID BARKAT²

Keywords: Double star induction machine, Balancing strategy, Five-level inverter, Direct torque control, Space vector modulation.

This paper concerns the study of direct torque control (DTC) based on space vector modulation for a double star induction machine fed by two five-level diode-clamped inverters. This control is proposed to solve the drawbacks of the conventional DTC based on electromagnetic torque and stator flux hysteresis controllers. In the case of multilevel inverters-based drive, the operation with unbalanced voltage in the dc-bus affects the drive performances due to the generation of uncharacteristic harmonics in each inverter output voltage as well as the presence of overvoltage across the semiconductors. For this reason, a DTC using capacitor voltage balancing strategy to maintain the neutral-point balance is presented. Simulation results, considering different work conditions, are presented to validate the good performance of the proposed control method.

1. INTRODUCTION

Multiphase machines have been proposed for different fields of industry that need high power such as electric hybrid vehicles, locomotive, traction and ship propulsion and other applications, which require safeness condition like aerospace and offshore wind energy system [1]. These machines exhibit several advantages over the conventional three-phase drives such as reduced torque ripple, reduced rotor harmonics as they can be filtered, reduced dc-link current harmonics content, and increased reliability as the large number of machine phases allows operation with one or more phase in fault [2].

One common example of multiphase machine is the double star induction machine (DSIM). The stator of this kind of machines is constituted by two windings with phases shifted from one another by an angle of 30 electrical degrees [3]. A six-phase two-level inverter commonly powers these windings.

Direct torque control (DTC) strategy is known by its simple decoupled scheme for stator flux and electromagnetic torque control. This control has more advantages like fast response and less dependency to machines parameters. However, due to its structure, the main problems of this method are the high level of torque and flux ripples and variable switching frequency [4].

Constant switching frequency DTC method using space vector modulation (SVM) has been proposed to face those problems. The direct torque control based on space vector modulation (DTC-SVM) replaces the switching table by voltage modulator responsible to generate switching signals for the voltage source inverter [5]. This type of system associated to the DSIM presents advantages to naval ship propulsion systems, which rely on high power quality and survivable drives [6,7].

The multilevel concept is used to decrease the harmonic distortion in the output waveforms without decreasing the inverter power output [8]. However, the integration of the multilevel DCI to improve the performance of the DTC-SVM is not a simple task and the circuit limitation of the DCI should be considered. One of the major problems of this topology is the balancing of the capacitor voltages. Indeed, when the capacitors are not balanced, the voltage in the neutral point can significantly fluctuate and may cause

malfunction or even failure of the switching devices due to overstress [9,10]. Several methods were proposed to overcome this problem; some of these methods were presented in [11,12]. The use of redundant states using SVM to balance the capacitor voltages is one of the most effective solutions that deal with voltage drift phenomenon in multilevel inverters [13].

The purpose of this work is to propose a five-level DTC-SVM method with efficient dc voltages balancing control method dedicated to double star induction machine-based drives. The proposed approach is different from that proposed in [12] since it is based on SVM instead of lookup table. The present paper is organized as follows: in second section the direct torque control based on space vector modulation with voltage balancing strategy principal is presented. In third section, a modeling of the DSIM is presented; a suitable transformation matrix is used to develop a simple dynamic model.

The proposed five-level DCI space vector modulation is presented in fourth section. The fifth section is reserved for dc-link balancing strategy. In sixth section, the DTC based on space vector modulation strategy is applied to get decoupled control of the stator flux and electromagnetic torque. In seventh section, simulation results of five-level DTC-SVM with balancing strategy are presented.

2. PRINCIPLE OF THE DTC-SVM USING VOLTAGE BALANCING STRATEGY

The block diagram of the DTC-SVM with balancing strategy scheme is shown in Fig. 1. Here, the torque and flux estimator block are used to determine the flux and the torque. Two PI controllers are used instead of switching table and hysteresis controllers. PI regulates flux and torque error giving reference voltage vector in x - y coordinates, which are transformed in α - β coordinates and delivered to SVM block.

¹ Department of Electrical Engineering, University of Kasdi Merbah, Ouargla 30000, BP. 511 Algeria, lakhdarbenyoussef@yahoo.com

² Faculty of Technology, Department of Electrical Engineering, University of M'sila, M'sila 28000, BP 166 Algeria.

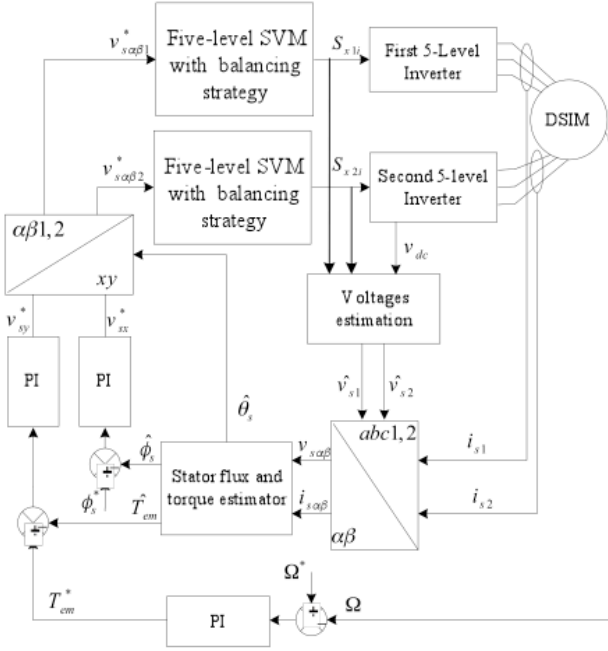


Fig. 1 – Five-level DTC-SVM of DSIM (with: $i = 1, 2, 3$ or 4).

3. DOUBLE STAR INDUCTION MACHINE MODELING

The stator voltage equations can be expressed as:

$$\begin{cases} v_{s1} = R_s i_{s1} + d\phi_{s1}, \\ v_{s2} = R_s i_{s2} + d\phi_{s2}, \end{cases} \quad (1)$$

with v_{s1}, v_{s2} are stator voltages of the first and second winding, i_{s1}, i_{s2} are stator currents of the first and second winding, and ϕ_{s1}, ϕ_{s2} are stator flux of the first and second winding.

The DSIM stator voltage equation (1) can be decomposed into three subsystems (α, β) , (z_1, z_2) and (z_3, z_4) , using the following transformation:

$$\begin{bmatrix} X_{s\alpha} & X_{s\beta} & X_{z1} & X_{z2} & X_{z3} & X_{z4} \end{bmatrix}^T = [A] \begin{bmatrix} X_s \end{bmatrix} \quad (2)$$

with $[X_s] = [X_{s1} \ X_{s2}]^T$, $[X_{s1}]^T = [X_{sa1} \ X_{sb1} \ X_{sc1}]^T$, $[X_{s2}]^T = [X_{sa2} \ X_{sb2} \ X_{sc2}]^T$, where X_s can refer to stator currents vector, stator flux vector, or stator voltages vector. The matrix A is given by:

$$[A] = \begin{bmatrix} \cos(0) & \cos\left(\frac{2\pi}{3}\right) & \cos\left(\frac{4\pi}{3}\right) & \cos(\gamma) & \cos\left(\frac{2\pi}{3} + \gamma\right) & \cos\left(\frac{4\pi}{3} + \gamma\right) \\ \sin(0) & \sin\left(\frac{2\pi}{3}\right) & \sin\left(\frac{4\pi}{3}\right) & \sin(\gamma) & \sin\left(\frac{2\pi}{3} + \gamma\right) & \sin\left(\frac{4\pi}{3} + \gamma\right) \\ \cos(0) & \cos\left(\frac{4\pi}{3}\right) & \cos\left(\frac{2\pi}{3}\right) & \cos(\pi - \gamma) & \cos\left(\frac{3\pi}{3} - \gamma\right) & \cos\left(\frac{5\pi}{3} - \gamma\right) \\ \sin(0) & \sin\left(\frac{4\pi}{3}\right) & \sin\left(\frac{2\pi}{3}\right) & \sin(\pi - \gamma) & \sin\left(\frac{3\pi}{3} - \gamma\right) & \sin\left(\frac{5\pi}{3} - \gamma\right) \\ 1 & 1 & 1 & 0 & 0 & 0 \\ 0 & 0 & 0 & 1 & 1 & 1 \end{bmatrix}, \quad (3)$$

where γ is the angle between the first stator and second stator. The stator voltage equations in the stator flux reference frame are given by:

$$\begin{cases} v_{sx} = R_s i_{sx} + d\phi_{sx} - p\Omega\phi_{sy}, \\ v_{sy} = R_s i_{sy} + d\phi_{sy} + p\Omega\phi_{sx}, \end{cases} \quad (4)$$

where v_{sx}, v_{sy} are x - y components of stator voltage, i_{sx}, i_{sy} are x - y components of stator current, ϕ_{sx}, ϕ_{sy} are x - y components of stator flux.

4. FIVE-LEVEL INVERTER MODELING AND ITS CONTROL

Figure 2 shows a three-phase five-level diode clamped inverter. The order of numbering of the switches for phase a is $(S_{ak1}, \dots, S_{ak8})$ and likewise for other two phases. The dc-bus consists of four capacitors acting as voltage divider. For a dc-bus voltage v_{dc} , the voltage across each capacitor is $v_{dc}/4$ and voltage stress on each device is limited to v_{dc} through clamping diodes [14].

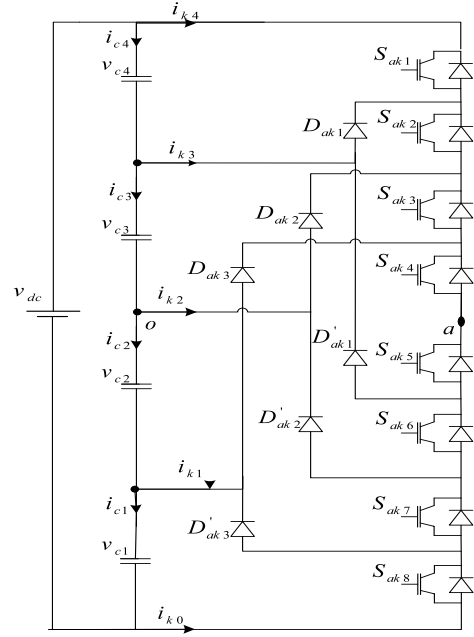


Fig. 2 – One phase-leg for a five-level DCI inverter ($k = 1$ for first inverter and $k = 2$ for second inverter).

The function F_{xki} describing the state of a switch S_{xki} is given by:

$$F_{xki} = \begin{cases} 1 & \text{if } S_{xki} \text{ is ON,} \\ 0 & \text{if } S_{xki} \text{ is OFF,} \end{cases} \quad (5)$$

with: $i = 1, \dots, 8$, $x = a, b, c$.

The five legs connections functions can be defined by:

$$\begin{cases} F_{cxk1} = F_{xk1} F_{xk2} F_{xk3} F_{xk4}, \\ F_{cxk2} = F_{xk2} F_{xk3} F_{xk4} F_{xk5}, \\ F_{cxk3} = F_{xk3} F_{xk4} F_{xk5} F_{xk1}, \\ F_{cxk4} = F_{xk4} F_{xk5} F_{xk1} F_{xk2}, \\ F_{cxk5} = F_{xk5} F_{xk1} F_{xk2} F_{xk3}. \end{cases} \quad (6)$$

The output voltages of five-level inverter can be written by:

$$\begin{bmatrix} v_{ak} \\ v_{bk} \\ v_{ck} \end{bmatrix} = \begin{bmatrix} F_{cak1} & F_{cak2} & F_{cak3} & F_{cak4} & F_{cak5} \\ F_{cbk1} & F_{cbk2} & F_{cbk3} & F_{cbk4} & F_{cbk5} \\ F_{cck1} & F_{cck2} & F_{cck3} & F_{cck4} & F_{cck5} \end{bmatrix} \begin{bmatrix} v_{c3} + v_{c4} \\ v_{c3} \\ 0 \\ v_{c2} \\ -(v_{c1} + v_{c2}) \end{bmatrix}. \quad (7)$$

The SVM technique is based on the generation of the reference voltage as an average voltage between the

possible discrete output voltages of the power inverter over a switching period. To do it, the control region of a converter is plotted considering their output voltages locating the switching states of the inverter. The determination of the switching sequence and the switching times is usually reduced to a geometrical search of the nearest state vectors to the reference vector in this control region every switching period [15].

The projection of the reference voltage vector in the first sector is presented in Fig. 3.

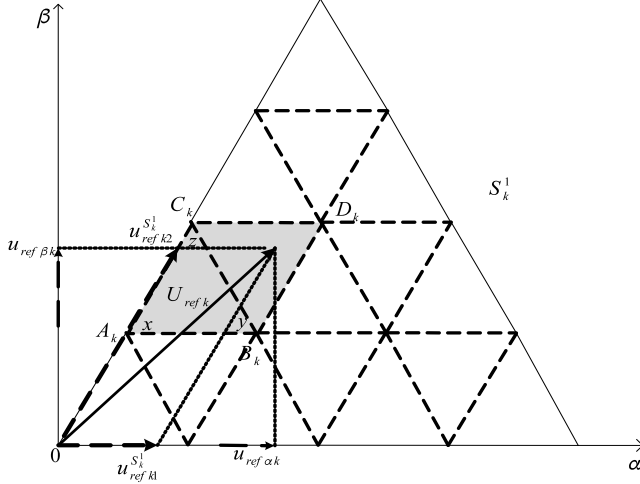


Fig. 3 – Projection of the reference voltage vector of a five-level DCI in the first sector.

The angle of the reference voltage is calculated by:

$$\vartheta_k = \tan^{-1} \left(\frac{u_{ref\beta k}}{u_{ref\alpha k}} \right) \quad (8)$$

The sector numbers are given by:

$$S_k^i = \text{ceil} \left(\frac{\vartheta_k}{\pi/3} \right) \in \{S_k^1, S_k^2, S_k^3, S_k^4, S_k^5, S_k^6\}, \quad (9)$$

where *ceil* is the C-function that adjusts any real number to the nearest one.

The two following entities are defined to determine the number of the triangle $\Delta_{qk}^{S_k^i}$ in a sector S_k^i :

$$\begin{cases} l_{k1}^{S_k^i} = \text{int}(u_{refk1}^{S_k^i}), \\ l_{k2}^{S_k^i} = \text{int}(u_{refk2}^{S_k^i}), \end{cases} \quad (10)$$

where *int* is a function that gives the whole part of a given real number.

According to Fig. 3, the coordinates of the tops A_k , B_k , C_k and D_k are given by:

$$\begin{cases} \left(u_{A_{k1}}^{\Delta_{qk}^{S_k^i}}, u_{A_{k2}}^{\Delta_{qk}^{S_k^i}} \right) = \left(l_{k1}^{S_k^i}, l_{k2}^{S_k^i} \right), \\ \left(u_{B_{k1}}^{\Delta_{qk}^{S_k^i}}, u_{B_{k2}}^{\Delta_{qk}^{S_k^i}} \right) = \left(l_{k1}^{S_k^i} + 1, l_{k2}^{S_k^i} \right), \\ \left(u_{C_{k1}}^{\Delta_{qk}^{S_k^i}}, u_{C_{k2}}^{\Delta_{qk}^{S_k^i}} \right) = \left(l_{k1}^{S_k^i}, l_{k2}^{S_k^i} + 1 \right), \\ \left(u_{D_{k1}}^{\Delta_{qk}^{S_k^i}}, u_{D_{k2}}^{\Delta_{qk}^{S_k^i}} \right) = \left(l_{k1}^{S_k^i} + 1, l_{k2}^{S_k^i} + 1 \right). \end{cases} \quad (11)$$

The application times are calculated by:

$$\begin{cases} t_{y_k}^{\Delta_{qk}^{S_k^i}} = \left(u_{refk1}^{S_k^i} - l_{k1}^{S_k^i} \right) T_s, \\ t_{z_k}^{\Delta_{qk}^{S_k^i}} = \left(u_{refk2}^{S_k^i} - l_{k2}^{S_k^i} \right) T_s, \\ t_{x_k}^{\Delta_{qk}^{S_k^i}} = T_s - \left(t_{y_k}^{\Delta_{qk}^{S_k^i}} + t_{z_k}^{\Delta_{qk}^{S_k^i}} \right). \end{cases} \quad (12)$$

where $t_{x_k}^{\Delta_{qk}^{S_k^i}}, t_{y_k}^{\Delta_{qk}^{S_k^i}}, t_{z_k}^{\Delta_{qk}^{S_k^i}}$ are the application times of the vectors $u_{x_k}^{\Delta_{qk}^{S_k^i}}, u_{y_k}^{\Delta_{qk}^{S_k^i}}, u_{z_k}^{\Delta_{qk}^{S_k^i}}$ respectively; with $q = 1, \dots, 16$ and $S_k^i = S_k^1, \dots, S_k^6$.

Table 1 gathers the various exchanges needed to be carried out between the phase currents in the first sector and phase currents in the other sectors.

Table 1

Interchanging phase currents between S_k^1 and $S_k^i, i = 2, \dots, 6$.

S_k^1	S_k^2	S_k^3	S_k^4	S_k^5	S_k^6
i_{ak}	$i_{ak} \rightarrow i_{bk}$	$i_{ak} \rightarrow i_{bk}$	$i_{ak} \rightarrow i_{ck}$	$i_{ak} \rightarrow i_{ck}$	i_{ak}
i_{bk}	$i_{bk} \rightarrow i_{ak}$	$i_{bk} \rightarrow i_{ck}$	i_{bk}	$i_{bk} \rightarrow i_{ak}$	$i_{bk} \rightarrow i_{ck}$
i_{ck}	i_{ck}	$i_{ck} \rightarrow i_{ak}$	$i_{ck} \rightarrow i_{ak}$	$i_{ck} \rightarrow i_{bk}$	$i_{ck} \rightarrow i_{bk}$

5. CAPACITORS VOLTAGES BALANCING STRATEGY

The core idea of this strategy is the minimization of a cost function using an appropriate selection of redundant switching states of the five-level DCI over a switching period [16].

The total energy of the four capacitors is given by:

$$E = \frac{1}{2} \sum_{j=1}^4 C_j v_{cj}^2 \quad (13)$$

where $C_1 = C_2 = C_3 = C_4 = C$.

The positive definite cost function is defined by:

$$J = \frac{1}{2} C \sum_{j=1}^4 \Delta v_{cj}^2, \quad (14)$$

where

$$\Delta v_{cj} = v_{cj} - v_{dc}/4. \quad (15)$$

The cost function can be minimized if the capacitor voltages are maintained at voltage reference values of ($v_{dc}/4$) [17]. The mathematical condition to minimize the cost function is:

$$dJ = \sum_{j=1}^4 \Delta v_{cj} i_{cj} \leq 0, \quad (16)$$

where i_{cj} is the current through the capacitor C_j .

The currents i_{cj} are affected by the dc-side intermediate branch currents i_{km} . So, the dc-capacitor currents are expressed as:

$$\begin{cases} i_{c4} = i_{c3} + \sum_{k=1}^2 i_{k3}, \\ i_{c2} = i_{c2} + \sum_{k=1}^2 i_{k2}, \\ i_{c2} = i_{c1} + \sum_{k=1}^2 i_{k1}. \end{cases} \quad (17)$$

The capacitor currents are given by:

$$i_{cj} = \frac{1}{4} \sum_{m=1}^3 m \left(\sum_{k=1}^2 i_{km}^{S_k^i} \right) - \sum_{m=j}^3 \left(\sum_{k=1}^2 i_{km}^{S_k^i} \right), \quad (18)$$

where $m=1, 2, 3$.

By substituting i_{cj} calculated from (18) in (16), the condition to achieve voltage balancing is deduced as:

$$\sum_{j=1}^4 \Delta v_{cj} \left(\frac{1}{4} \sum_{m=1}^3 m \left(\sum_{k=1}^2 i_{km}^{S_k^i} \right) - \sum_{m=j}^3 \left(\sum_{k=1}^2 i_{km}^{S_k^i} \right) \right) \leq 0. \quad (19)$$

Since the net dc-link voltage is regulated at v_{dc} it results:

$$\sum_{j=1}^4 \Delta v_{cj} = 0. \quad (20)$$

By substituting Δv_{c4} calculated from (20) in (19) it yields

$$\sum_{j=1}^3 \Delta v_{cj} \left(\sum_{m=1}^3 \left(\sum_{k=1}^2 i_{km}^{S_k^i} \right) \right) \geq 0. \quad (21)$$

The application of the average operator, over one sampling period, to (21) results in:

$$\frac{1}{T} \sum_{KT}^{(K+1)T} \Delta v_{cj} \left(\sum_{m=1}^3 \left(\sum_{k=1}^2 i_{km}^{S_k^i} \right) \right) dt \geq 0. \quad (22)$$

Capacitor voltages can be regarded as constants [15], and consequently the equation (22) is simplified to:

$$\sum_{j=1}^3 \Delta v_{cj}(K) \left(\sum_{m=1}^3 \left(\sum_{k=1}^2 i_{km}^{S_k^i}(K) \right) \right) dt \geq 0, \quad (23)$$

with $\Delta v_{cj}(K)$ is the voltage drifts of C_j at sampling period K ; $\bar{i}_{km}^{S_k^i}(K)$ is the average value of the j^{th} dc-side intermediate branch current.

To calculate $\bar{i}_{km}^{S_k^i}(K)$, representing the contributions of switching states to the dc side intermediate branch, the relationships between the dc and ac side currents $\bar{i}_{k3}^{S_k^i}, \bar{i}_{k2}^{S_k^i}$ and $\bar{i}_{k1}^{S_k^i}$ are required.

$$\begin{bmatrix} \bar{i}_{k3}^{S_k^i} \\ \bar{i}_{k2}^{S_k^i} \\ \bar{i}_{k1}^{S_k^i} \end{bmatrix} = \frac{1}{T} \begin{bmatrix} i_{k3x}^{S_k^i} & i_{k3y}^{S_k^i} & i_{k3z}^{S_k^i} \\ i_{k2x}^{S_k^i} & i_{k2y}^{S_k^i} & i_{k2z}^{S_k^i} \\ i_{k1x}^{S_k^i} & i_{k1y}^{S_k^i} & i_{k1z}^{S_k^i} \end{bmatrix} \begin{bmatrix} t_{kx}^{\Delta_q^{S_k^i}} \\ t_{ky}^{\Delta_q^{S_k^i}} \\ t_{kz}^{\Delta_q^{S_k^i}} \end{bmatrix}, \quad (24)$$

where $i_{kmx}^{S_k^i}, i_{kmy}^{S_k^i}, i_{kmz}^{S_k^i}$ are the charging currents switching states related to the x_k, y_k and z_k in the triangle $\Delta_q^{S_k^i}$

minimizing the function cost J_k .

6. DIRECT TORQUE CONTROL BASED ON SPACE VECTOR MODULATION

The presented control strategy is based on simplified stator voltage equations described in stator flux-oriented x - y coordinates as follows:

$$\begin{cases} v_{sx} = R_s i_{sx} + d\phi_s, \\ v_{sy} = R_s i_{sy} + \omega_s \phi_{sx}, \end{cases} \quad (25)$$

where ω_s is the speed of the stator flux reference.

The electromagnetic torque expression is simplified to:

$$\hat{T}_{em} = p |\hat{\phi}_s| i_{sy}. \quad (26)$$

The stator flux magnitude and its angle are estimated by:

$$\begin{cases} |\hat{\phi}_s| = \sqrt{\hat{\phi}_{s\alpha}^2 + \hat{\phi}_{s\beta}^2}, \\ \hat{\theta}_s = \text{atan}\left(\frac{\hat{\phi}_{s\beta}}{\hat{\phi}_{s\alpha}}\right). \end{cases} \quad (27)$$

To transform the stator voltages from the stator flux reference frame x - y to the stationary reference α - β , the following rotation transformation is adopted:

$$\begin{cases} \begin{bmatrix} v_{s\alpha 1}^* \\ v_{s\beta 1}^* \end{bmatrix} = [P(\hat{\theta}_s)] \begin{bmatrix} v_{sx}^* \\ v_{sy}^* \end{bmatrix}, \\ \begin{bmatrix} v_{s\alpha 2}^* \\ v_{s\beta 2}^* \end{bmatrix} = [P(\hat{\theta}_s - \gamma)] \begin{bmatrix} v_{sx}^* \\ v_{sy}^* \end{bmatrix}, \end{cases} \quad (28)$$

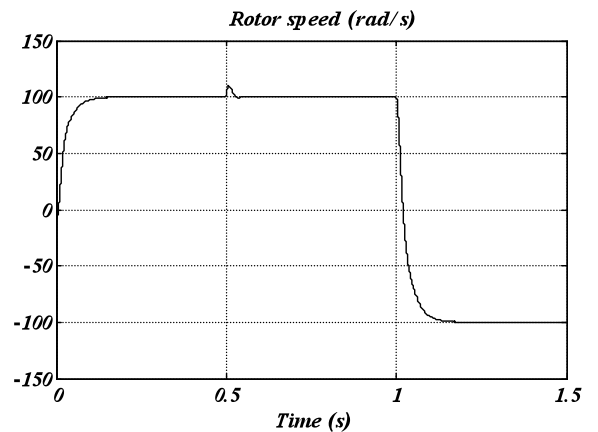
with

$$[P(\hat{\theta}_s)] = \begin{bmatrix} \cos(\hat{\theta}_s) & -\sin(\hat{\theta}_s) \\ \sin(\hat{\theta}_s) & \cos(\hat{\theta}_s) \end{bmatrix}.$$

7. SIMULATION RESULTS

The simulation results are obtained using the following dc-link capacitors values $C_1 = C_2 = C_3 = C_4 = C = 1$ mF. The dc side of the inverter is supplied by a constant dc source of $v_{dc} = 600$ V.

The drive is started with full load torque of 10 N.m, in which the DSIM is accelerated from standstill to reference speed 100 rad/s. Afterwards, a step variation on the load torque to 0 N.m is applied at time 0.5 s. After that, a sudden reversion in the speed command from 100 rad/s to -100 rad/s is introduced at 1s. Indeed, Fig. 4 presents the simulation results of the five-level DTC-SVM of DSIM.



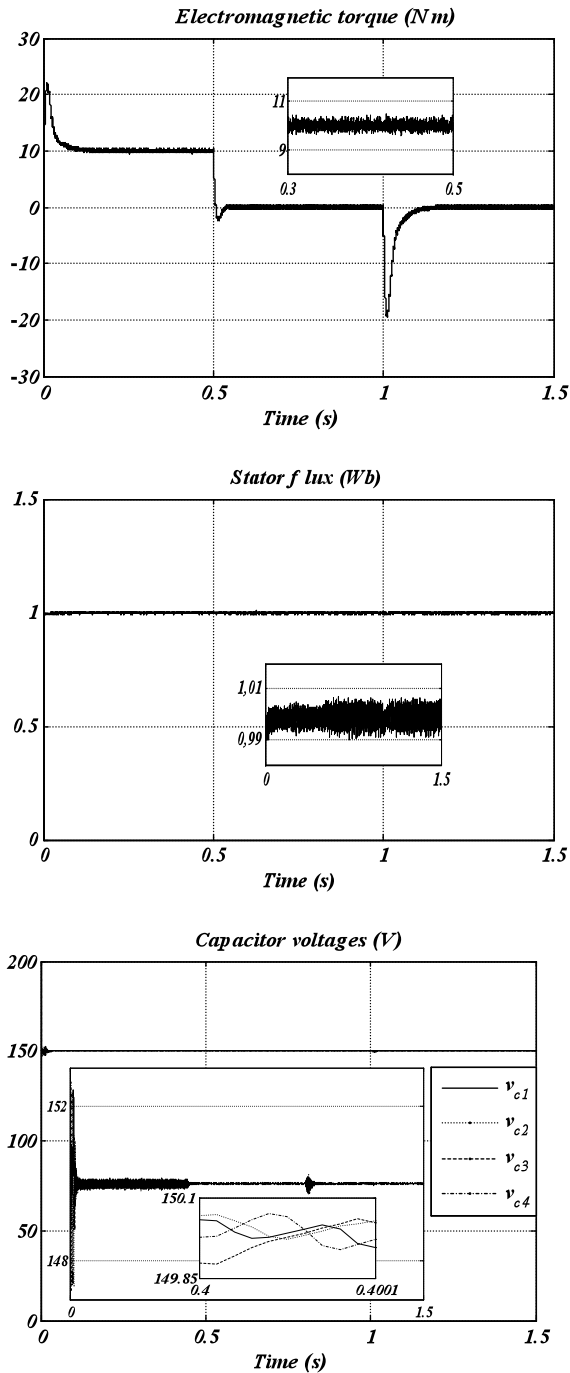


Fig. 4 – Dynamic responses of five-level DTC-SVM with balancing strategy for DSIM.

Simulation results show that the rotor speed follows its reference value, and the stator flux is very similar to the nominal case. Moreover, the decoupling control between torque and stator flux is always confirmed. The input voltages of the five-level DCI are balanced around 150 V. This result stresses the importance of the inverter input dc voltages balancing strategy incorporated into the multilevel space vector modulation algorithm.

8. CONCLUSION

In this paper, the performance of the direct torque control based on space vector modulation of DSIM fed by two five-level DCI has been highlighted. Simulation results show the effectiveness of the adopted control scheme. Indeed, a high performance and quick torque response are obtained in

different tests such as load torque variation and speed reference reversion. Moreover, the proposed DTC-SVM presents reduced flux and torque ripples. However, the control of the multilevel DCI leads to a higher complexity in the modulation algorithm because the balancing dc-link voltage task is an additional constrained to fulfill. Note that, the five-level DCI controlled by DTC-SVM endowed by a balancing strategy is an effective way to balance the input capacitor voltages of both multilevel inverters.

Received on September 26, 2019

APPENDIX

The parameters of DSIM are given in Table 2.

Table 2

DSIM parameters.

1 kW, 2 poles, 220 V, 50 Hz		
Quantity	Symbol	Value
Stator resistance	R_s	4.67 W
Rotor resistance	R_r	8 W
Stator inductance	L_s	0.374 H
Rotor inductance	L_r	0.374 H
Mutual inductance	M	0.365 H
Inertia moment	J	0.003 kgm ²

REFERENCES

1. K. Nounou, M. Benbouzid, K. Marouani, J. Frédéric, A. Kheloui, *Performance comparison of open-circuit fault-tolerant control strategies for multiphase permanent magnet machines for naval applications*, *Electrical Engineering*, **100**, 3, pp. 1827–1836, 2018.
2. L. Yuan, H. Bing, K. Wei, L. Ying, *A novel current vector decomposition controller design for six-phase permanent magnet synchronous motor*, **23**, 4, pp. 841–849, 2016.
3. H. Kouki, F. Mouldi, H. Rehaouia, *Harmonic analysis of SVPWM control strategy on VSI-fed double-star induction machine performances*, *Electrical Engineering*, **98**, 2, pp. 133–143, 2016.
4. W. Zheng, W. Xueqing, C. Jiawei, C. Ming, H. Yihua, *Direct torque control of T-NPC inverters-fed double-stator-winding PMSM drives with SVM*, *IEEE Transaction on Power Electronics*, **33**, 2, pp. 1541–1553, 2018.
5. Z. Zhifeng, T. Renyuan, B. Baodong, X. Dexin, *Novel direct torque control based on space vector modulation with adaptive stator flux observer for induction motors*, *IEEE Transaction on Magnetics*, **46**, 8, pp. 3133–3136, 2010.
6. A. Khedher, M. Mimouni, *Sensorless-adaptive DTC of double star induction motor*, *Energy Conversion and Management* **51**, pp. 2878–2892, 2010.
7. V. Talaeizadeh, R. Kianinezhad, S. Seyfossadat, H. Shayanfar, *Direct torque control of six-phase induction motors using three-phase matrix converter*, *Energy Conversion and Management*, **51**, pp. 2482–2491, 2010.
8. N. Susheela, P. Kumar, S. Sharma, *Generalized algorithm of reverse mapping based SVPWM strategy for diode-clamped multilevel inverters*, *Transaction on Industry Applications*, **54**, 3, pp. 2425–2437, 2018.
9. B. Sergio, F. Alber, A. Salvador, C. Alejandro, *A modulation strategy to operate multilevel multiphase diode-clamped dc-sc converters at low frequency modulation indices with dc-link capacitor voltage balance*, *IEEE Transaction on Power Electronics*, **32**, 10, pp. 7521–7533, 2017.
10. B. Sergio, G. Robert, N. Joan, B. Joseb, *Decoupled DC-link capacitor voltage control of DC-AC multilevel multileg converters*, *IEEE Transaction on Industrial Electronics*, **63**, 3, pp. 1344–1349, 2016.
11. R. Chibani, E. Berkouk, M. Boucherit, *Five-level NPC VSI: different ways to balance input DC link voltages*, *Elektrika*, **11**, 1, pp. 19–33, 2009.

12. E. Benyoussef, S. Barkat, *Five-level direct torque control with balancing strategy of double star induction machine*, International Journal of Systems Applications, Engineering & Development, **14**, pp. 116–123, 2020.
13. L. Wuhua, H. Jiawei, H. Senjun, Y. Heya, Y. Huan, H. Xiangning, *Capacitor voltage balance control of five-level modular composited converter with hybrid space vector modulation*, IEEE Transaction on Power Electronics, **33**, 7, pp. 5629–5640, 2018.
14. R. Pawar, R. Nagpure, *Five-level diode clamped multilevel inverter (DCMLI) based electric spring for smart grid applications*, Energy Procedia, **117**, pp. 862–869, 2017.
15. M. Mazuela, I. Baraia, S. Alain, E. Ivan, I. Torre, A. Inigo, *Dc-link voltage balancing strategy based on SVM and reactive power exchange for 5L-MPC back-to-back converter for medium-voltage drives*, IEEE Transaction on Industrial Electronics, **63**, 12, pp. 7864–7875, 2016.
16. P. Zhiguo, Z. Fang, A. Keith, R. Victor, M. John, G. Slobodan, *Voltage balancing control of diode-clamped multilevel rectifier/inverter systems*, IEEE Transactions on Industry Applications, **41**, 6, pp. 1698–1706, 2005.
17. H. Hotait, A. Massoud, S. Finney, B. Williams, *Capacitor voltage balancing using redundant states of space vector modulation for five-level diode clamped inverters*, IEEE Institution of Engineering and Technology, **3**, 2, pp. 292–313, 2010.